

## Complex band structure in neutron-deficient $^{178}\text{Hg}$

F. G. Kondev,<sup>1</sup> M. P. Carpenter,<sup>1</sup> R. V. F. Janssens,<sup>1</sup> I. Wiedenhöver,<sup>1</sup> M. Alcorta,<sup>1</sup> P. Bhattacharyya,<sup>2</sup> L. T. Brown,<sup>1,3</sup> C. N. Davids,<sup>1</sup> S. M. Fischer,<sup>4</sup> T. L. Khoo,<sup>1</sup> T. Lauritsen,<sup>1</sup> C. J. Lister,<sup>1</sup> R. Nouicer,<sup>5</sup> W. Reviol,<sup>6</sup> L. L. Riedinger,<sup>6</sup> D. Seweryniak,<sup>1</sup> S. Siem,<sup>1,7</sup> A. A. Sonzogni,<sup>1</sup> J. Uusitalo,<sup>1</sup> and P. J. Woods<sup>8</sup>

<sup>1</sup>Argonne National Laboratory, Argonne, Illinois 60439

<sup>2</sup>Purdue University, West Lafayette, Indiana 47907

<sup>3</sup>Vanderbilt University, Nashville, Tennessee 37235

<sup>4</sup>DePaul University, Chicago, Illinois 60614

<sup>5</sup>University of Illinois at Chicago, Chicago, Illinois 60607

<sup>6</sup>University of Tennessee, Knoxville, Tennessee 37996

<sup>7</sup>University of Oslo, Oslo, Norway

<sup>8</sup>Department of Physics, University of Edinburgh, Edinburgh EH9 3JZ, United Kingdom

(Received 27 September 1999; published 16 December 1999)

Using the GAMMASPHERE array in conjunction with the Fragment Mass Analyzer, the level structure of the near drip-line nucleus  $^{178}\text{Hg}$  has been considerably expanded with the recoil-decay tagging technique. Of particular interest is a new rotational band which exhibits a complex decay towards the low spin states arising from both the prolate-deformed and the nearly spherical coexisting minima. It is proposed that this band is associated at low spin with an octupole vibration which is crossed at moderate frequency by a shape driving, two quasiproton excitation.

PACS number(s): 27.70.+q, 23.20.Lv, 23.60.+e, 25.70.Gh

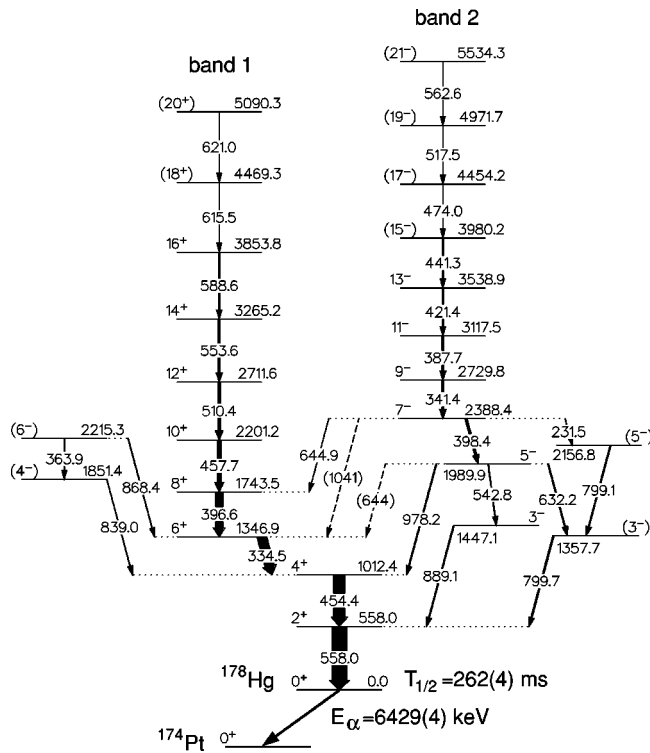
The first few states along the yrast lines of the near drip-line isotopes  $^{176,178}\text{Hg}$  have only recently been identified [1,2]. The observation of levels in these nuclei is hampered by (i) fission, which dominates the heavy-ion induced fusion cross section and results in a large, unwanted background, and by (ii) fragmentation into many channels of the small remaining evaporation-residue cross section. These severe experimental challenges are addressed by combining the ability of a recoil separator to discriminate the residues from the unwanted reaction products with the recoil-decay tagging (RDT) technique, where in-beam  $\gamma$  rays emitted in the decay of excited states in a nucleus of interest are correlated with the subsequent charged-particle decay of the ground or isomeric state. The studies of Refs. [1,2], together with the earlier work on  $^{180}\text{Hg}$  by Dracoulis *et al.* [3], have validated the mean-field calculations of Refs. [4,5] by demonstrating that below neutron number  $N=102$  (mid-shell) the excitation energy of a rotational band built on a prolate, normal deformed shape ( $\beta_2 \sim 0.25$ ) increases with decreasing mass to the point where there is no longer any clear evidence for its presence at low spin in  $^{176}\text{Hg}$ . Furthermore, the data also confirm the prediction that for  $N < 100$  the coexisting oblate ground state evolves steadily as a function of decreasing  $N$  towards a spherical shape.

The susceptibility of the Hg isotopes to shape changes is well documented. For example, besides the oblate-prolate shape coexistence alluded to above, which has now been traced from  $N=96$  to  $N=110$  [1,2,6], excitations associated with collective oblate ( $\beta_2 \sim -0.15$ ) [7], noncollective prolate ( $\gamma = -120^\circ$ ) [8], and superdeformed ( $\beta_2 \sim 0.5$ ) [9] shapes have been established in the heavier Hg isotopes ( $A \geq 189$ ). Furthermore, in the lighter Hg nuclei there is evidence that the occupation of certain orbitals impacts the nuclear shape significantly. Specifically, Ma *et al.* [10] have shown in  $^{186}\text{Hg}$  that the occupation of specific neutron orbit-

als drives the nucleus towards a so-called intermediate prolate deformation, i.e., a deformation lying midway between those associated with the normal deformed and superdeformed minima. Thus, it appears worthwhile to explore the neutron-deficient Hg nuclei further in order to determine the type of excitations they can sustain at low and medium spin. Such a study is motivated also by the calculations of Ref. [5] which predict specific shape changes as a function of excitation energy in these neutron-deficient nuclei.

The present paper reports on a new study of  $^{178}\text{Hg}$ . By taking advantage of the high detection efficiency of the GAMMASPHERE multidetector array [11] and of the capabilities of the Fragment Mass Analyzer (FMA) [12] to select evaporation residues of interest, it was possible to extend considerably the  $^{178}\text{Hg}$  level structure. The prolate-deformed yrast cascade has been traced up to  $I=20\hbar$  and a new band of negative parity has been found. The latter stands out by the complexity of its decay towards the yrast and near-yrast states, by the magnitude of its moments of inertia, and by the presence at low rotational frequency of strong alignment effects.

The experimental techniques under which the present data were collected are in many ways similar to those described in Refs. [1,13]. Briefly, a 350-MeV  $^{78}\text{Kr}$  beam from the ATLAS superconducting linear accelerator was delivered to a  $\sim 0.5$  mg/cm<sup>2</sup> self-supporting  $^{103}\text{Rh}$  target, where the  $^{178}\text{Hg}$  nuclei of interest were produced via the  $p2n$  reaction channel. Prompt gamma rays were detected with the 101 Compton-suppressed Ge spectrometers of the GAMMASPHERE array. Recoiling evaporation residues were dispersed according to their mass-to-charge ( $M/Q$ ) ratio by the FMA. The position and energy loss information at the focal plane was measured with a position-sensitive parallel-grid avalanche counter (PGAC). The residues were subsequently implanted in a 40 mm  $\times$  40 mm, 60- $\mu\text{m}$ -thick



double-sided Si strip detector (DSSD) located 40 cm behind the PGAC. This DSSD was used not only to detect the implantation of a residue and to determine its time of arrival with respect to the prompt  $\gamma$ -ray flash detected by GAMMASPHERE, but also to measure its subsequent  $\alpha$  decay(s). The  $40 \times 40$  pixel segmentation of the DSSD provided effective spatial and time correlations between the implants and the  $\alpha$  decays. A total of  $1.4 \times 10^8$  coincidence events were written to tape either when two or more GAMMASPHERE detectors fired in coincidence with the PGAC and/or DSSD counters (implant event), or when a charged-particle decay was detected in the DSSD (decay event).

Approximately 32% of all the mass-selected coincidence events were associated with  $^{178}\text{Hg}$ . The GAMMASPHERE data were sorted in prompt coincidence matrices and cubes gated in several ways on the information from the PGAC and the DSSD. In general, the most stringent coincidence relationships involved the correlation with mass 178 and the 6.43-MeV characteristic  $\alpha$  decay line [14]. Most of the gamma rays presented in the level scheme of Fig. 1 were established from such data. However, for the weakest transitions, coincidence events gated only on mass 178 were also used. This approach takes advantage of the higher statistics of these data, while relying on the power of the high-fold coincidence relationships to provide unambiguous placements. Sample coincidence spectra are shown in Fig. 2 for

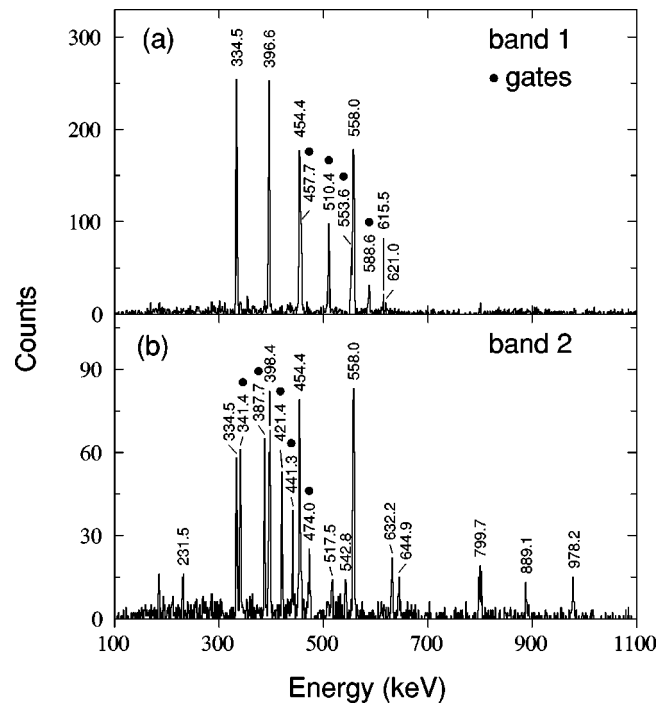


FIG. 2. Sample spectra obtained from the RDT-gated coincidence data for bands 1 (top) and 2 (bottom). The spectra are sums of coincidence gates placed on the transitions marked with the black dots.

the two main sequences seen in the experiment. Information on the multipolarity of the transitions was deduced from mass- and  $\alpha$ -gated angular distribution data. For the weaker  $\gamma$  rays,  $I_\gamma(34^\circ)/I_\gamma(90^\circ)$  anisotropy ratios were used instead, where data from adjacent rings were summed together to produce spectra corresponding to average angles of  $34^\circ$  (and the symmetric angle of  $146^\circ$ ) and  $90^\circ$  with respect to the beam direction (further details will be given in Ref. [15]).

When compared to the work of Ref. [1], the prolate band has been extended by four transitions up to the  $I^\pi = (20^+)$  state. The placement and ordering of the transitions are based on the observed coincidence relationships and on the measured relative intensities. Their stretched  $E2$  character was derived from the measured angular distributions and anisotropy ratios, thereby confirming the spin values given in Fig. 1. The multipolarity of the transitions depopulating the two highest levels in the band could not be established directly because of the weak intensities involved. Nevertheless, the assignments can be viewed as likely because of the collective character of the sequence. A similar argument holds for the top transitions in a second rotational sequence (band 2), which was also firmly established from the coincidence data (Fig. 1). The  $E2$  character of the lower spin transitions in this band is firmly established from the measured angular distributions. Remarkably, the decay out of band 2 towards the lower states is fragmented over a fair number of pathways, most of which feed levels that have not been reported previously. The odd spin, negative parity assignment to this band comes from the measured multipolarity of the main decay-out transitions (398.4, 644.9, 889.1, 978.2 keV), and from the requirement that the character of each transition be

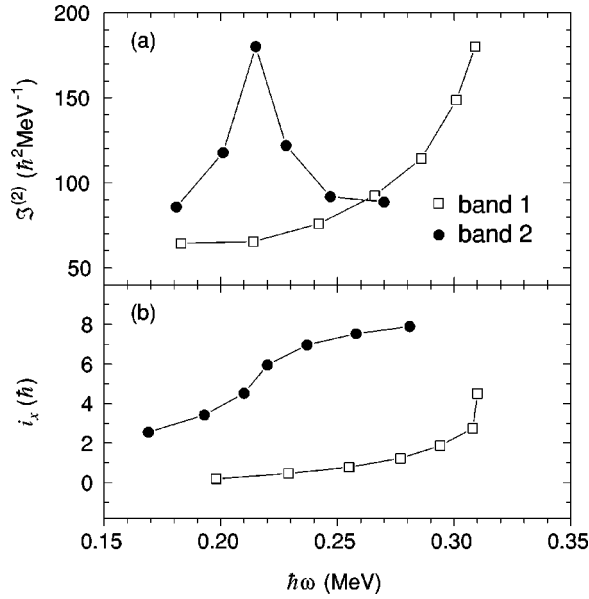


FIG. 3. Aligned spins  $i_x$  and  $\mathcal{J}^{(2)}$  moment of inertia for bands 1 and 2 in  $^{178}\text{Hg}$ . In both cases a common reference was subtracted, with the Harris parameters  $J_0 = 29\hbar^2 \text{ MeV}^{-1}$ ,  $J_1 = 200\hbar^4 \text{ MeV}^{-3}$ .

restricted to either  $E1$ ,  $E2$ ,  $M1$ , or to the appropriate mixing of these multipolarities. In particular, only  $I = 7\hbar$  is possible for the 2388.4 keV level, as any other spin value implies the presence of at least one higher-order ( $E3$  or  $M3$ )  $\gamma$  ray. A positive parity is deemed unlikely as a 1041 keV  $M1$  transition would be expected to be four times stronger than the competing 644.9 keV  $\gamma$  ray (energy factor). In contrast, as discussed in detail below, the  $I^\pi = 7^-$  assignment agrees with systematics based on a comparison with negative parity bands in the neighboring isotones.

Figure 3 compares the aligned spins,  $i_x$ , and the dynamic moments of inertia,  $\mathcal{J}^{(2)}$ , as a function of rotational frequency,  $\hbar\omega$ , for the prolate-deformed yrast sequence and for the newly discovered negative parity cascade. As can be seen from the figure, the data for band 1 extend into the frequency range where the first band crossing occurs. The characteristic crossing frequency ( $\hbar\omega_c \sim 0.31 \text{ MeV}$ ) is essentially the same as that measured for the first backbending in the isotone  $^{176}\text{Pt}$  [16]. In both nuclei, as in all their neighbors, this first crossing can be associated with the alignment of a pair of  $i_{13/2}$  neutrons [16,17].

Band 2 exhibits a few unusual properties: (a) its alignment at low frequency is  $\sim 3\hbar$ ; (b) it undergoes a subsequent alignment gain of roughly  $5\hbar$  at the noticeably low frequency of 0.21 MeV; (c) at low spin, its  $\mathcal{J}^{(2)}$  moment is  $\sim 25\%$  larger than the corresponding value in band 1; and (d) it stands out by the complexity of its deexcitation pattern as the  $7^-$  state decays into three (possibly four) levels. This may suggest that the associated intrinsic structure is quite different from that of band 1 and that the decay proceeds towards most, if not all, available lower-energy levels without much selection on the basis of shape or degree of collectivity. In some respects, band 2 in  $^{178}\text{Hg}$  shows striking similarities with band 3 of  $^{186}\text{Hg}$  reported by Ma *et al.* [10]. The

latter structure, extending from  $11^-$  to  $31^-$ , was found to decay to levels associated with both oblate (ground-state) and normal-deformed prolate deformations. The band is also characterized by a larger  $\mathcal{J}^{(2)}$  moment than any other  $^{186}\text{Hg}$  collective structure, and by the largest average  $i_x$  value. It has been interpreted as an excitation of two quasi-neutrons, either the  $\nu^2([651]1/2 \otimes [514]7/2)$  or the  $\nu^2([651]1/2 \otimes [771]1/2)$  configuration, or a combination of both, intruding from above the  $N = 126$  shell. The measured quadrupole moment  $Q_0 = 11(2)e b$  [10] highlights the shape-driving effects of these neutron orbitals: the resulting deformation  $\beta_2 = 0.34(4)$  is intermediate between those associated with the normal-deformed and the superdeformed shapes. As in Ref. [10], total Routhian surface [18] and cranked shell model calculations based on a Woods-Saxon potential [19] were used to ascertain whether similar neutron configurations can play a role in  $^{178}\text{Hg}$ . It was found that, with the eight fewer neutrons than in  $^{186}\text{Hg}$ , the shape driving orbitals mentioned above are located far above the Fermi surface and, as a result, do not establish a yrast shape of intermediate deformation. The cranking calculations also show that the lowest neutron excitations of negative parity involve the  $i_{13/2}$  orbital. The presence of a single  $i_{13/2}$  neutron blocks any low-frequency crossing and, hence, it is difficult to account for the sudden gain in alignment seen in the data of Fig. 3. Thus, it appears unlikely that band 2 can be readily associated with a neutron excitation.

In nuclei of this mass region, two quasiproton configurations have often been considered candidates for the description of the lowest negative parity excitations. In fact, Ma *et al.* [10] discussed the  $\pi^2(i_{13/2} \otimes h_{9/2})$  configuration as a possible candidate for the  $^{186}\text{Hg}$  negative parity band described above. While at  $N = 106$  ( $^{186}\text{Hg}$ ) this configuration is higher in energy than the neutron excitations considered above, it becomes energetically favored when  $N$  decreases. The total Routhian surface calculations indicate that this two quasiproton excitation, labeled by the Nilsson asymptotic quantum numbers  $\pi^2([660]1/2^+ \otimes [541]1/2^-)$ , drives  $^{178}\text{Hg}$  from its yrast deformation of  $\beta_2 = 0.24$ ,  $\gamma = -6^\circ$  towards a slightly more deformed shape with a larger degree of triaxiality;  $\beta_2 = 0.27$ ,  $\gamma = 15^\circ$ . With the orbitals involved, the eight units of alignment measured experimentally at high frequency are accounted for [20]. However, it should be realized that this  $\pi^2(i_{13/2} \otimes h_{9/2})$  excitation is not the only possible one. In particular, from studies of the light, odd-even Au isotopes [21–23], the  $[530]1/2^-$  state (of predominant  $f_{7/2}$  parentage) has also been identified. Hence, a  $\pi^2(i_{13/2} \otimes f_{7/2})$  two quasiproton configuration cannot be ruled out. Furthermore, sizable mixing between these  $\pi^2(i_{13/2} \otimes h_{9/2})$  and  $\pi^2(i_{13/2} \otimes f_{7/2})$  configurations is also possible.

The nature of the low spin states in band 2 and the interpretation of the low-frequency band crossing can also be addressed. In this mass region, low-spin, negative parity band structures have sometimes been interpreted as rotational bands built on octupole vibrations [24]. The initial alignment value of  $i_x = 3\hbar$  measured for band 2 is in agreement with expectations for an octupole phonon. In addition, as can be seen in Fig. 1, one of the main decay branches out of the lowest state in band 2 is the 644.9 keV,  $7^- \rightarrow 8^+$

transition. It has a larger intensity than the competing  $E1$  transition (1041 keV) linking the  $7^-$  and  $6^+$  levels. The situation is similar to that seen in the  $^{174}\text{Os}$  [25] and  $^{176}\text{Pt}$  isotones [16], and in the neighboring  $^{178}\text{Pt}$  [15] and  $^{176-180}\text{Os}$  nuclei [26], where an interpretation in terms of an octupole vibration has also been invoked. Hence, within this scenario, the sudden gain in alignment seen in the data results from the crossing of an octupole rotational band with a two quasiproton excitation. The microscopic structure of the octupole phonon is probably rather complex with contributions of various orbitals fulfilling the  $\Delta j = \Delta l = 3$  condition. It is likely, however, that the proton  $i_{13/2} - f_{7/2}$  coupling will be an important component as both orbitals lie close to the Fermi surface. If so, the shape driving effects of the  $i_{13/2}$  orbital described above will remain strong and the nuclear shape associated with the low-spin part of band 2 may well be similar to the one associated with the two quasiproton configuration. This, in turn, would provide a qualitative explanation for the large  $\mathcal{J}^{(2)}$  moment of inertia and the fragmented decay observed at low spin in band 2.

To summarize, the selectivity of the RDT technique has been combined with the high detection efficiency of GAMMASPHERE to obtain an expanded level scheme for the neutron-deficient  $^{178}\text{Hg}$  nucleus. Of particular interest is a negative parity, odd-spin band exhibiting a sharp alignment

gain at low frequency and a complex decay towards lower spin states. It is proposed that this sequence is associated with a rotational band based on an octupole vibration which is crossed by a shape-driving two quasiproton configuration. It would be of interest to establish whether a cascade with similar characteristics occurs in the neighboring  $^{176}\text{Hg}$  and  $^{180}\text{Hg}$  nuclei or whether it is restricted solely to  $^{178}\text{Hg}$  [27]. In any event, the present results demonstrate further that a near drip-line Hg isotope, such as  $^{178}\text{Hg}$ , is as susceptible to shape changes as heavier Hg nuclei. Nevertheless, despite the sensitivity of the present measurements, the discovery of the  $^{178}\text{Hg}$  superdeformed band predicted by Nazarewicz [5] remains a challenge which will, hopefully, be addressed by future experiments.

The authors express their gratitude to the staff of the ATLAS accelerator for the quality of the beam and to the members of the Physics Support Group for their assistance in the preparation of the experiment. Numerous discussions with W. Nazarewicz, P.-H. Heenen, G.D. Dracoulis, and M.A. Riley are gratefully acknowledged. One of us (S.S.) acknowledges support from a NATO grant through the Research Council of Norway. This work was supported by the U.S. Department of Energy, Nuclear Physics Division, under Contract Nos. W-31-109-ENG-38 and DE-FG02-96ER40983.

- 
- [1] M. P. Carpenter *et al.*, Phys. Rev. Lett. **78**, 3650 (1997).  
 [2] M. Muikku *et al.*, Phys. Rev. C **58**, R3033 (1998).  
 [3] G. D. Dracoulis *et al.*, Phys. Lett. B **208**, 365 (1988).  
 [4] R. Bengtsson, T. Bengtsson, J. Dudek, G. Leander, W. Nazarewicz, and J.-Y. Zhang, Phys. Lett. B **183**, 1 (1987).  
 [5] W. Nazarewicz, Phys. Lett. B **305**, 195 (1993).  
 [6] J. L. Wood, K. Heyde, W. Nazarewicz, M. Huyse, and P. Van Duppen, Phys. Rep. **251**, 101 (1992), and references therein; J. H. Hamilton, Prog. Part. Nucl. Phys. **28**, 87 (1992), and references therein.  
 [7] H. Hübel, A. P. Byrne, S. Ogaza, A. E. Stuchbery, G. D. Dracoulis, and M. Guttormsen, Nucl. Phys. **A453**, 313 (1986).  
 [8] D. Ye *et al.*, Phys. Lett. B **236**, 7 (1990).  
 [9] R. V. F. Janssens and T. L. Khoo, Annu. Rev. Nucl. Part. Sci. **41**, 321 (1991).  
 [10] W. C. Ma *et al.*, Phys. Rev. C **47**, R5 (1993).  
 [11] I. Y. Lee, Nucl. Phys. **A520**, 641c (1990).  
 [12] C. N. Davids, B. B. Back, K. Bindra, D. J. Henderson, W. Kutschera, T. Lauritsen, Y. Nagame, P. Sugathan, A. V. Ramayya, and W. B. Walters, Nucl. Instrum. Methods Phys. Res. B **70**, 358 (1992).  
 [13] M. P. Carpenter, Z. Phys. A **358**, 261 (1997).  
 [14] Y. A. Akaoli, Nucl. Data Sheets **84**, 1 (1998).  
 [15] F. G. Kondev *et al.* (unpublished).  
 [16] B. Cederwall *et al.*, Z. Phys. A **337**, 283 (1990).  
 [17] R. Wyss, W. Satula, W. Nazarewicz, and A. Johnson, Nucl. Phys. **A511**, 324 (1990).  
 [18] R. Wyss (private communication).  
 [19] W. Nazarewicz, J. Dudek, R. Bengtsson, T. Bengtsson, and I. Ragnarsson, Nucl. Phys. **A435**, 397 (1985), and references therein.  
 [20] This  $\pi^2([660]1/2^+ \otimes [541]1/2^-)$  configuration has also been identified in  $^{182,184,186}\text{Pt}$ . See M. P. Carpenter *et al.*, Nucl. Phys. **A513**, 125 (1990); D. G. Popescu *et al.*, Phys. Rev. C **55**, 1175 (1997).  
 [21] F. G. Kondev *et al.* (unpublished).  
 [22] W. F. Mueller *et al.*, Phys. Rev. C **59**, 2009 (1999); A. J. Larabee, M. P. Carpenter, L. L. Riedinger, L. H. Courtney, J. C. Waddington, V. P. Janzen, W. Nazarewicz, J.-y. Zhang, R. Bengtsson, and G. Leander, Phys. Lett. **169B**, 21 (1986).  
 [23] W. F. Mueller, Ph.D. thesis, University of Tennessee, 1997 (unpublished).  
 [24] G. D. Dracoulis, J. Phys. (Paris) Suppl. **C10**, c10 (1980).  
 [25] B. Fabricius, G. D. Dracoulis, R. A. Bark, A. E. Stuchbery, T. Kibedi, and A. M. Baxter, Nucl. Phys. **A511**, 345 (1990).  
 [26] G. D. Dracoulis, C. Fahlander, and M. P. Fewell, Nucl. Phys. **A383**, 119 (1982).  
 [27] It is interesting to note that the  $^{176}\text{Hg}$  level scheme of M. Muikku *et al.* [2] reports two levels outside the main yrast sequence which may well represent the lower members of a band similar in nature to the structure discussed in the present work.